Phase Transitions and Crystal Structure of Dimethylammonium Tribromomercurate(II), $(CH_3)_2NH_2HgBr_3$, as Studied by ^{81}Br NQR and Single Crystal X-ray Diffraction*

Hiromitsu Terao[a], Masao Hashimoto[b], Tsutomu Okuda[c], and Alarich Weiss †

[a] Department of Chemistry, Faculty of Integrated Arts and Sciences, Tokushima University, Minamijosanjima-cho, Tokushima 770, Japan
[b] Department of Chemistry, Faculty of Science, Kobe University, Nadaku, Kobe 657, Japan
[c] Department of Chemistry, Faculty of Science, Hiroshima University, Kagamiyama, Higashihiroshima 724, Japan

Z. Naturforsch. **53 a,** 559–567 (1998); received January 26, 1998

The temperature dependence of the ^{81}Br NQR frequencies of the title compound has revealed the presence of three phases (I, II and III, in the order of decreasing temperature): T_{c1} (II - I) = (318 ± 10) K and T_{c2} (III - II) = (202 ± 1) K. The transitions were confirmed by thermal analysis (DTA). Both of the II-I and I-II transitions exhibited strong hysteresis (*i. e.,* superheating and supercooling, respectively). The crystal data, determined by single crystal X-ray diffraction, are: monoclinic, space group P2/a, a = 1384.8(3), b = 934.7(4), c = 1452.0(2) pm, β = 104.10(1)°, Z = 8, R = 0.076. The crystal has two crystallographically independent cations $(CH_3)_2NH_2^+$ and an infinite chain of anions almost in the c-direction. The anion chain is considered to consist of a $HgBr_2$ molecule and two different $HgBr_4^{2-}$ anions which are interconnected *via* weak intermolecular Hg···Br bonds. The splitting patterns of the ^{81}Br NQR spectra indicate that rearrangements of the Hg-Br bonds are slight at the III-II transition but serious at the II-I transition. Some of the ^{81}Br NQR lines show anomalous temperature coefficients, attributable probably to thermal motions of cations.

Key words: $(CH_3)_2NH_2HgBr_3$; X-Ray Analysis; NQR; Phase Transition; Crystal Structure.

Introduction

A general tendency has been found for the coordination of Hg(II) in the complex compounds of HgX_2 (X = Cl, Br, I). That is, the Hg(II) atoms like to take a linear two coordination in chloride complexes and a tetrahedral coordination in iodide ones, while the coordination in bromide complexes is of intermediate nature. A wide variety of structures has thus been encountered in the compounds $R_xNH_{4-x}HgBr_3$ (R = alkyl group). For example, a trigonal planar coordination, which is usually extended to a tetrahedral or a trigonal bipyramidal coordination by forming one or two extra intermolecular Hg···X bonds, has often been found. In addition to the interest on the crystal structure, one can also expect for this type of compounds phase transitions associated with the thermal motion of the cations.

In the present study on dimethylammonium tribromomercurate(II) $(CH_3)_2NH_2HgBr_3$ we have applied ^{81}Br NQR, thermal analysis (DTA), and single crystal X-ray diffraction to elucidate the crystal structure, chemical bonding, and possible phase transitions. The crystal structures of the related compounds $(CH_3)_2NH_2HgCl_3$ and $[(CH_3)_2NH_2]_2HgBr_4$ have already been reported by Ben Salah, *et al.* [1] and Pabst *et al.* [2], respectively. In the former crystal there exists an interesting chain of anions in which each of three independent Hg(II) atoms has two short terminal Hg-Cl bonds and two long bridging Hg-Cl bonds, and nine Cl atoms are left chemically independent. In the latter crystal, however, a discrete distorted $HgBr_4^{2-}$ tetrahedron has been found instead of the chain structure.

* Presented at the XIVth International Symposium on Nuclear Quadrupole Interactions, Pisa, Italy, July 20–25, 1997.

Reprint requests to Dr. H. Terao;
E-mail: terao@ias.tokushima-u.ac.jp.

0932-0784 / 98 / 0600-0559 $ 06.00

Table 1. Experimental conditions for the crystal structure determination and crystallographic data of $(CH_3)_2NH_2HgBr_3$.

Formula		$C_2H_8Br_3HgN$
Formula weight		486.39
Crystal habit		Prismatic (colorless)
Size/(mm)^3		0.1×0.25×0.3
Absorption coeff. (μ/m^{-1})		30039
Diffractometer		Rigaku AFC5R
Wavelength		71.069 pm (MoK_α)
Monochrometer		Graphite (002)
Scan		$\omega/2\theta$
$(\sin\theta/\lambda)_{max}$/pm^{-1}		0.0054
Reflections measured		2682
Symmetry independent		2561
Considered $F_0 > 3\sigma(F_0)$		1017
Number of free parameters		101
$F(000)$		1696.00
$R(F)$		0.076
$R_w(F)$		0.061
Lattice constants	a/pm	1384.8(3)
	b/pm	934.7(4)
	c/pm	1452.0(2)
	β/°	104.10(1)
$V_{ucell}\times10^{-6}$/(pm)^3		1822.7(8)
Space group		C_{2h}^4 - P2/a
Formula units/Unit cell (Z)		8
ρ_{calc}/mg·m^{-3}		3.545
ρ_{obs}/mg·m^{-3}		3.36
Point positions		x, y, z; $\frac{1}{2}+x, -y, z$; $-x, -y, -z$; $\frac{1}{2}-x, y, -z$

Table 2. ^{81}Br NQR frequencies in each phase of $(CH_3)_2NH_2HgBr_3$ at representative temperatures.

Phase III (77K)	Phase II (298 K)	Phase I (320 K)
145.31	137.02	130.32
143.38	133.90	125.27
142.48	95.00	122.52
141.65	90.65	119.47
93.54	82.90	117.09
93.33	60.44	114.57
92.35		69.20
89.84		66.44
86.70		47.28
83.46		
66.50		
65.55		

Experimental

The crystals of $(CH_3)_2NH_2HgBr_3$ were prepared from a dilute hydrobromic acid solution containing stoichiometric amounts of $HgBr_2$ and $(CH_3)_2NH_3Br$ obtained by adding a hydrobromic acid to an aqueous solution of $(CH_3)_2NH_2$. The C, H, and N analyses were consistent with the chemical formula; found/calc.; weight %: C: 5.01/5.00; H: 0.68/0.42; N: 2.82/2.92.

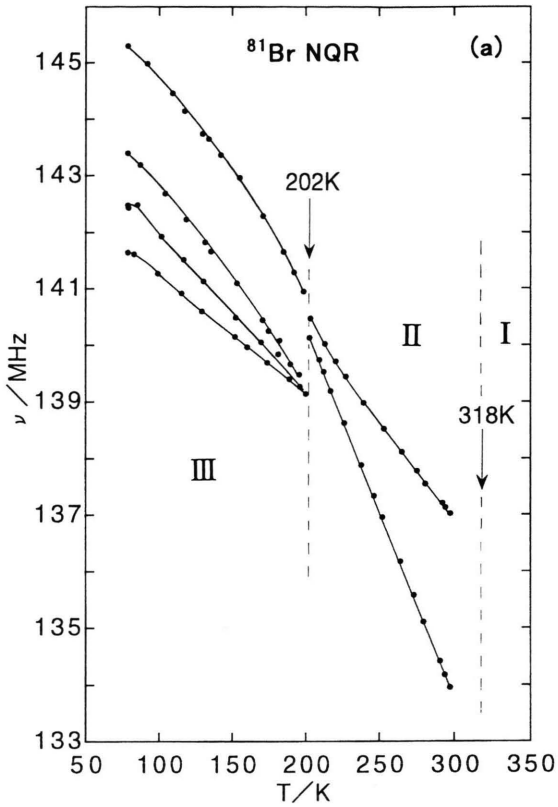

Fig. 1. Temperature dependence of ^{81}Br NQR frequencies in the phases II and III of $(CH_3)_2NH_2HgBr_3$; (a) high-frequency lines.

The ^{81}Br NQR spectra were obtained with a super-regenerative spectrometer. The signals were recorded on a recorder through a lock-in amplifier with Zeeman modulation. The accuracy of the frequency measurements is estimated to be within ± 0.02 MHz. The temperature of the sample was measured by a Cu-constantan thermocouple with an estimated accuracy within ±1 K. The DTA measurements were done by using a home made apparatus.

Details of the single crystal X-ray experiment are summarized in Table 1. The structure was solved by the direct method [3] and refined by the full matrix least squares method [4]. Non-hydrogen atoms, except for N(2) and C(2-4), which were refined isotropically, were refined with anisotropic thermal factors. Hydrogen atoms were included in the least squares calculations but not refined. The crystallographic data are given in Table 1.

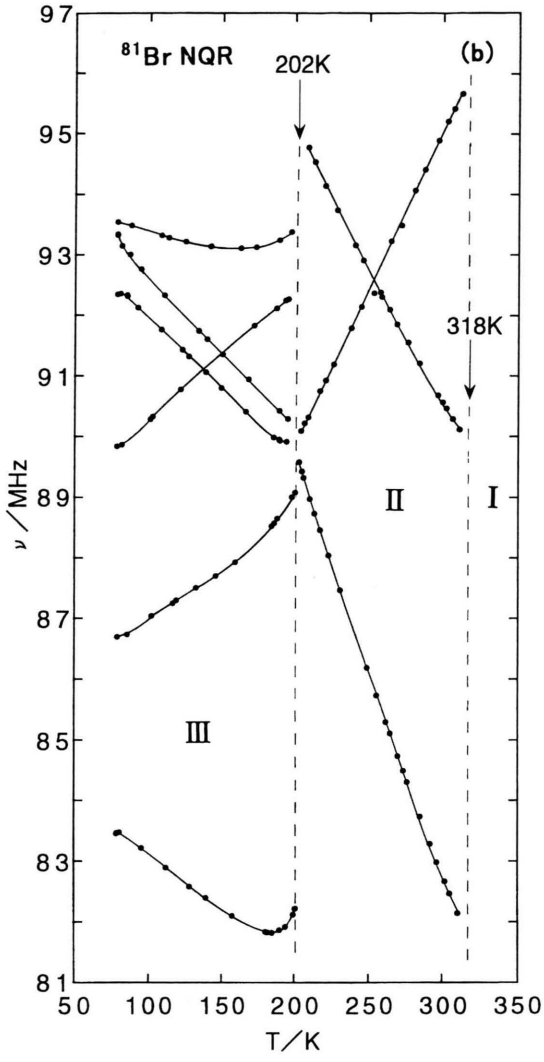

Fig. 2. Temperature dependence of ^{81}Br NQR frequencies in the phases II and III of $(CH_3)_2NH_2HgBr_3$; (b) middle-frequency lines.

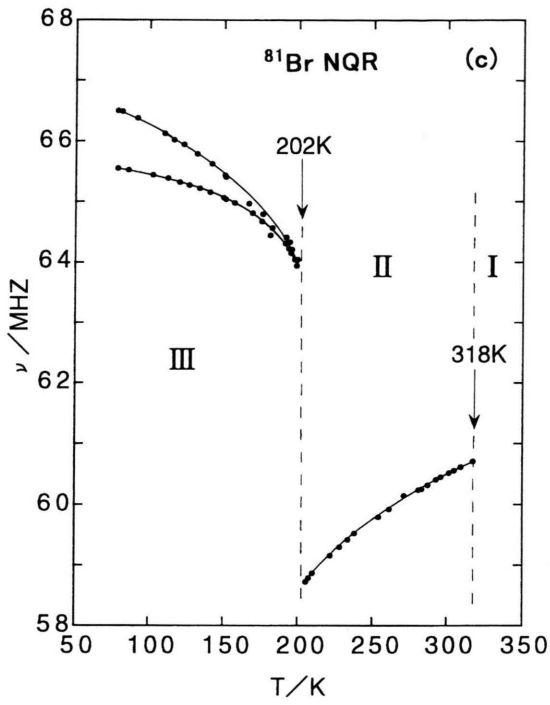

Fig. 3. Temperature dependence of ^{81}Br NQR frequencies in the phases II and III of $(CH_3)_2NH_2HgBr_3$; (c) low-frequency lines.

Results

^{81}Br NQR Spectra

The temperature dependence of the ^{81}Br NQR frequencies in the phases II and III and that in phase I are shown in Figs. 1 - 3 and Figs. 4 - 6, respectively. These figures indicate the occurrence of phase transitions at T_{c1} = (318 ± 10) K and T_{c2} = (202 ± 1) K . The ^{81}Br NQR frequencies in each phase at the representative temperatures are listed in Table 2. Twelve, six, and nine resonance lines have been observed for the low temperature phase (III), the room temperature phase (II), and the high temperature phase (I), respectively. At T_{c2} (the III-II transition), the temperature dependence curves are discontinuous, indicating a 1st-order phase transition. The II-I transition at T_{c1} is also of 1st-order, judging from the discontinuity in the frequency *vs.* temperature curves. Phase I is supercooled on cooling with no difficulty. When phase I was supercooled to 77 K, no signals were detected, while on subsequent heating the resonance lines appeared at $T > ca.$ 110 K (Figs. 4 - 6). The supercooled phase I was transformed in few hours to phase II when the sample was kept at *ca.* –20 °C. T_{c1} is very dependent on the thermal history of the samples; it tends to become lower for the sample which experienced the II-I transition. It is notable that some of the frequency *vs.* temperature curves of each phase exhibit anomalous temperature coefficients.

DTA Measurement

The representative DTA curves are depicted in Figs. 7 and 8. In Fig. 7 the exothermic peak at 196 K

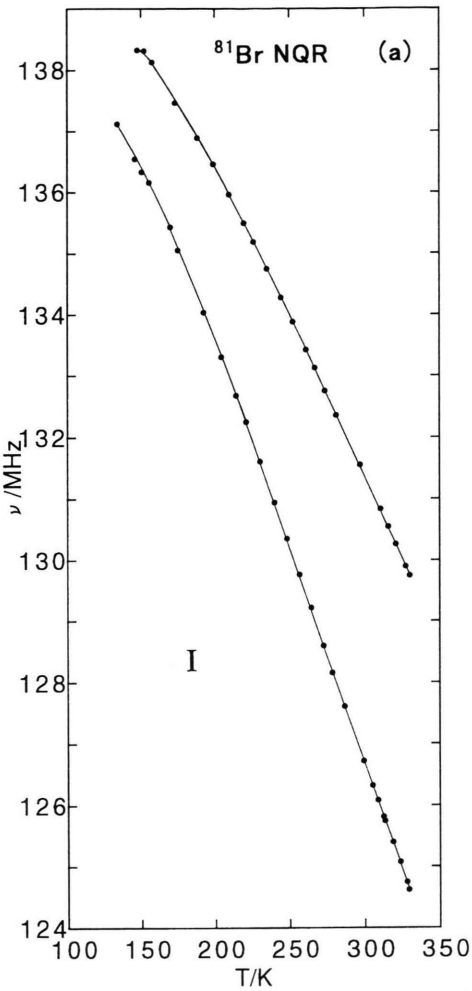

Fig. 4. Temperature dependence of ^{81}Br NQR frequencies in the phase I of $(CH_3)_2NH_2HgBr_3$; (a) high-frequency lines.

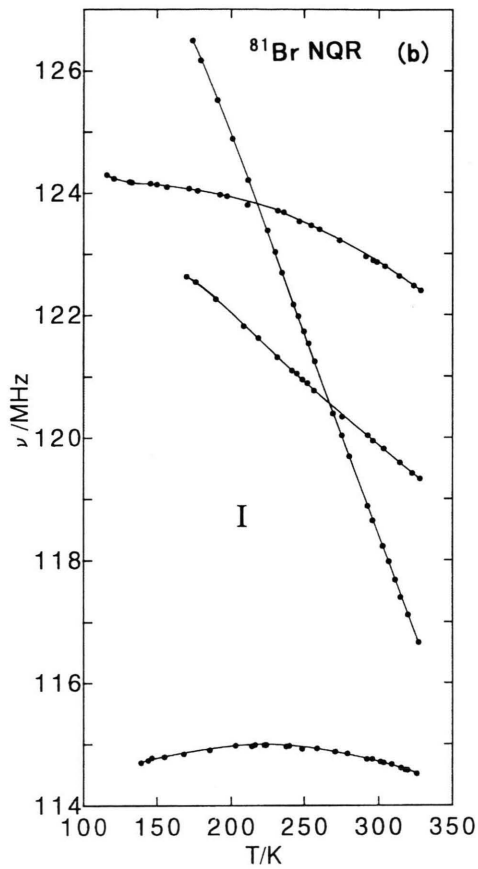

Fig. 5. Temperature dependence of ^{81}Br NQR frequencies in the phase I of $(CH_3)_2NH_2HgBr_3$; (b) middle-frequency lines.

on cooling (Run 1) and the endothermic one at 199 K on heating (Run 2) are ascribed to the II-III and III-II transitions, respectively. The small discrepancy in the transition temperatures indicates a 1st-order transition. Run 3 in Fig. 8 is the DTA curve of a sample which had not experienced the II-I transition, and Run 5 is the curve of a sample which had experienced the II-I transition a few times. Thus, the transition temperature is very dependent on the history of samples, as stated above. This phenomenon indicates that the II-I transition is superheated considerably if the seeds of phase I were not created in phase II through the experience of the transition. The exothermic peak corresponding to the I-II transition was not observed because phase I was always supercooled (Run 4). The melting point is deduced as 374 K from the DTA curve (Run 6).

The Crystal Structure of the Room Temperature Phase (Phase II)

In Table 3 the atomic coordinates and the thermal parameters are listed. Table 4 contains distances and angles in the ions and selected interionic distances. Short N···Br contacts (343 and 349 pm) are found, as listed in the table. Figure 9 shows the crystal structure.

The structure consists of two crystallographically independent cations $(CH_3)_2NH_2^+$ and an infinite chain of anions arranged almost in the *c*-direction. There exist three crystallographically independent Hg atoms, two of which, Hg(2) and Hg(3), are located on the two-fold axes. As shown in Fig. 10, the chain of anions is formed by sharing of Br(3) or Br(4) atoms

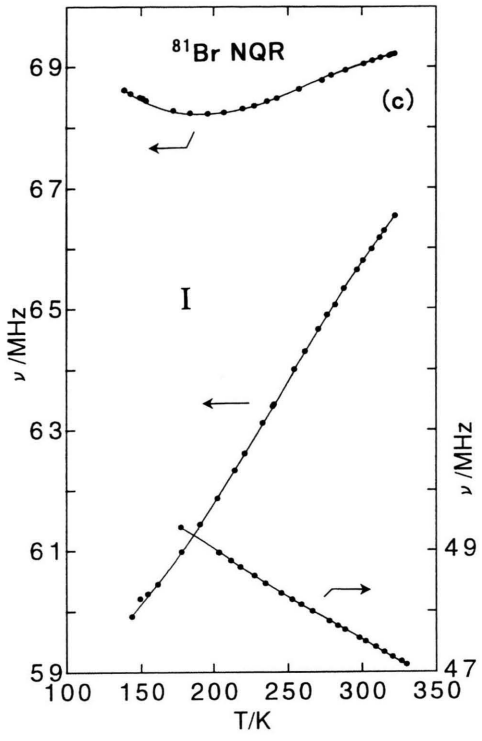

Fig. 6. Temperature dependence of ^{81}Br NQR frequencies in the phase I of $(CH_3)_2NH_2HgBr_3$; (c) low-frequency lines.

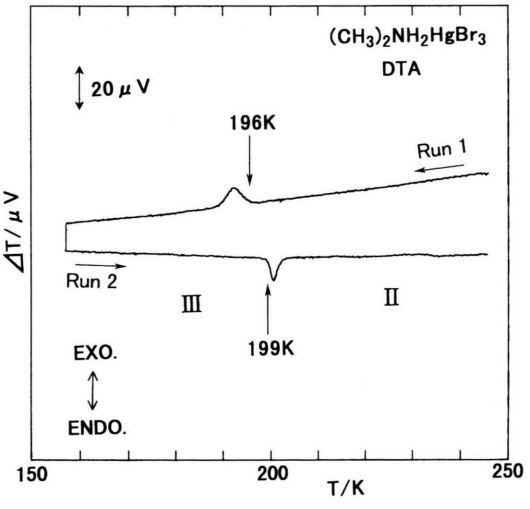

Fig. 7. The representative DTA curves observed at the phase transition between the phases II and III.

which are situated at the two corners of each of the three distinct heavily distorted $HgBr_4$ polyhedra, so that six Br atoms remain as crystallographically and hence chemically different in the crystal. The magnitude of the thermal parameters for the N(2) atom indicates a large amplitude thermal motion of the cation (Table 3).

Table 3. Positional and thermal parameters $B_{eq}/B^*_{iso}/(pm)^2$. Estimated standard errors in parentheses.

Atom	*x/a*	*y/b*	*z/c*	$B_{eq}/B^*_{iso} \times 10^{-4}$
Hg(1)	0.3452(2)	–0.2089(3)	0.7648(2)	5.82(9)
Hg(2)	0.2500	0.2217(4)	1.0000	4.2(1)
Hg(3)	0.2500	–0.3075(4)	0.5000	4.5(1)
Br(1)	0.4353(5)	–0.0584(8)	0.6772(4)	5.3(2)
Br(2)	0.2944 (5)	–0.3823 (7)	0.8698(4)	4.5(2)
Br(3)	0.1514(5)	–0.2015(8)	0.6116(4)	4.7(2)
Br(4)	0.2818(5)	0.0698(7)	0.8546(4)	4.8(2)
Br(5)	0.0821(4)	0.3374(7)	0.9241(4)	4.5(2)
Br(6)	0.1161(5)	0.5181(8)	0.3945(4)	6.0(2)
N(1)	0.542(5)	0.278(6)	0.902 (4)	6(2)
C(1)	0.498(5)	0.313(9)	0.806(5)	8(3)
N(2)	0.100(5)	0.297(9)	0.597(5)	13(2)*
C(2)	0.573(5)	0.138(8)	0.916(4)	6(1)*
C(3)	0.142(5)	0.176(8)	0.567(5)	8(2)*
C(4)	0.148(5)	0.374(7)	0.676 (4)	7(2)*

Discussion

The ^{81}Br NQR Spectra and the Structure of Phase II

In accordance with the crystal structure, six ^{81}Br NQR resonance lines have been observed in phase II. The observed resonance lines exist in a remarkably wide frequency range (60 ~ 140 MHz), indicating extreme chemical differences among the Br atoms. In $HgBr_4$ polyhedra (Fig. 10), Hg(1) has two short (243.4 and 244.3 pm) and two long (304.0 and 313.2 pm) bonds, while Hg(2) and Hg(3) have four bonds which are less different in bond lengths (255.8 to 266.8 pm). Therefore, the anion chain may be considered to consist of a $HgBr_2$ "molecule" and two different $HgBr_4^{2-}$ anions, which are interconnected *via* weak Hg(1)···Br(3) and Hg(1)···Br(4) bonds. Then, the two NQR lines at extremely high frequency can be assigned to Br(1) and Br(2), and the remaining four lines to the Br atoms in the two kinds of $HgBr_4^-$, each of which contains two chemically different Br atoms. Interestingly, two of the lines assigned to $HgBr_4^-$ exhibit anomalous positive temperature coefficients, while the other two exhibit normal negative but a little steep ones. A positive temperature dependence has often been observed for the Br atoms concerned with the hydrogen bonds such as N-H···Br (*e.g.* in

Table 4. Intra- and interatomic distances and angles in the structure of $(CH_3)_2NH_2HgBr_3$. The distances d are given in pm and the angles in degree.

Connection	*d*/pm	Connection	Angle/°
Hg(1)-Br(1)	243.4(6)	Br(1)-Hg(1)-Br(2)	166.2(3)
Hg(1)-Br(2)	244.3(6)	Br(1)-Hg(1)-Br(3)	94.5(2)
Hg(1)-Br(3)	304.0(7)	Br(1)-Hg(1)-Br(4)	88.2(2)
Hg(1)-Br(4)	313.2(7)	Br(2)-Hg(1)-Br(3)	97.8(2)
Hg(2)-Br(4)	266.8(6)	Br(2)-Hg(1)-Br(4)	98.0(2)
Hg(2)-Br(5)	255.8(6)	Br(3)-Hg(1)-Br(4)	89.9(2)
Hg(3)-Br(3)	255.9(6)	Br(4)-Hg(2)-Br(4')	115.7(3)
Hg(3)-Br(6)	265.6(7)	Br(4)-Hg(2)-Br(5)	101.0(2)
N(1)-C(1)	142(7)	Br(5)-Hg(2)-Br(5')	130.0(3)
N(1)-C(2)	137(7)	Br(3)-Hg(3)-Br(3')	134.5(3)
N(2)-C(3)	138(8)	Br(3)-Hg(3)-Br(6')	101.4(2)
N(2)-C(4)	138(8)	Br(6)-Hg(3)-Br(6')	104.3(4)
N(1)···Br(2')	366(5)	Hg(1)-Br(3)-Hg(3)	86.7(2)
N(1)···Br(2")	377(5)	Hg(1)-Br(4)-Hg(2)	152.7(3)
N(1)···Br(5')	343(4)	C(1)-N(1)-C(2)	114(6)
N(1)···Br(5")	364(6)	C(3)-N(2)-C(4)	122(8)
N(2)···Br(1')	358(7)		
N(2)···Br(6")	349(7)		
N(2)···Br(6"')	364(7)		

Br(3'), Br(6'): $\frac{1}{2} - x, y, 1 - z$; Br(4'), Br(5'): $\frac{1}{2} - x, y, 2 - z$; Br(2'): $1 - x, -y, 2 - z$; Br(2"): $-\frac{1}{2}, -y, z$; Br(5"): $-\frac{1}{2} + x, 1 - y, z$; Br(1'): $\frac{3}{2} + x, 1 - y, 1 + z$; Br(6"): $-x, -y, 1 - z$; Br(6"'): $x, y, 1 + z$.

$(CH_3NH_3)_2HgBr_4$ [5] and $CH_3CH_2NH_3HgBr_3$ [6]). With the activation of thermal motion of cations at higher temperatures the H-bonds will weaken, which will result in the increase in the NQR frequencies of Br atoms concerned. We expect two fairly strong H-bonds in N(1)···Br(5) (343 pm) and N(2)···Br(6) (349 pm) contacts (Table 4). Thus, Br(5) and Br(6) may be assigned to the resonance lines with the positive temperature coefficients. Then the remaining two lines may be assigned to the Br(3) and Br(4) atoms *i. e.* the bridging atoms.

It is interesting to compare the relationship between the NQR frequencies and the bond lengths in the present and related compounds. In $KHgBr_3 \cdot H_2O$ [7] we find a $HgBr_4$ polyhedron which is very similar to the $Hg(1)Br_4$ in the present crystal. In the crystal of $KHgBr_3 \cdot H_2O$ there is a zigzag chain consisting of anion polyhedra which have two shorter, almost equal terminal bonds (249.7 pm) and two longer equal bridging bonds (283.6 pm), the angle between the terminal Hg-Br bonds being 148.0°. Thus the chain may be considered to be approximately composed of $HgBr_2$ and Br^-. The ^{81}Br NQR frequencies of $KHgBr_3 \cdot H_2O$ at room temperature are 114.21 and 113.12 MHz for the terminal Br atoms and 56.31

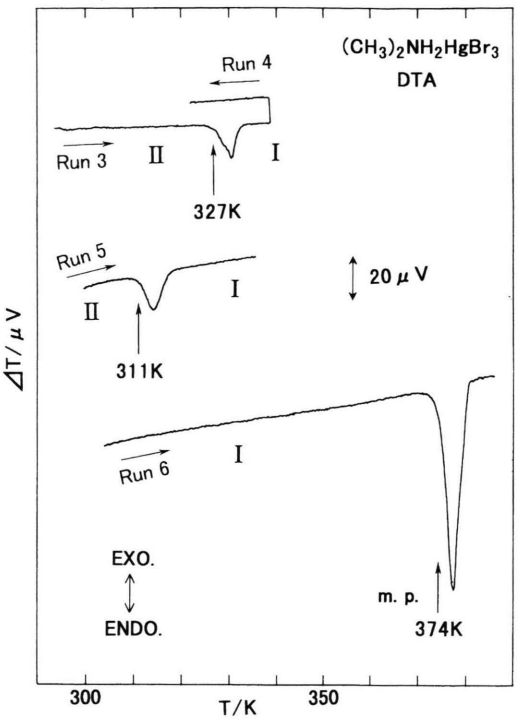

Fig. 8. The representative DTA curves observed at the phase transition between the phases I and II.

MHz for the bridging Br atom. In comparison with these, the Hg(1)-Br(1) and Hg(1)-Br(2) bond lengths are 243.4 and 244.3 pm and the ^{81}Br NQR frequencies of these Br atoms are 137 and 134 MHz. Therefore $HgBr_2$ units are recognized more clearly in $(CH_3)_2NH_2HgBr_3$ than in $KHgBr_3 \cdot H_2O$. On the one hand, the Hg-Br bond lengths and the ^{81}Br NQR frequencies found for $HgBr_4^{2-}$ in $(CH_3NH_3)_2HgBr_4$ are 2.591, 2.601, 2.602 and 2.602 pm [8], and 76.03, 81.72, 84.30 and 84.51 MHz [5], respectively. Those values in $[(CH_3)_2NH_2]_2HgBr_4$ which also contains $HgBr_4^{2-}$ are 2.588, 2.569, 2.603 and 2.650 pm [2], and 69.41, 79.71, 89.79 and 91.48 MHz [9], respectively. When these bond lengths and the ^{81}Br NQR frequencies are compared to those in $(CH_3)_2NH_2HgBr_3$, one can recognize the existence of $HgBr_4^{2-}$ units in this compound. On the other hand, an almost planar $HgBr_3^-$ has been found in *e.g.* $CH_3NH_3HgBr_3$ [10]. In this crystal the Hg atom completes its trigonal bipyramidal $HgBr_5$ configuration with extra intermolecular Hg···Br bonds, resulting in two terminal Br atoms and one bridging Br atom; the Hg-Br bond distances and ^{81}Br NQR frequencies are 252.7

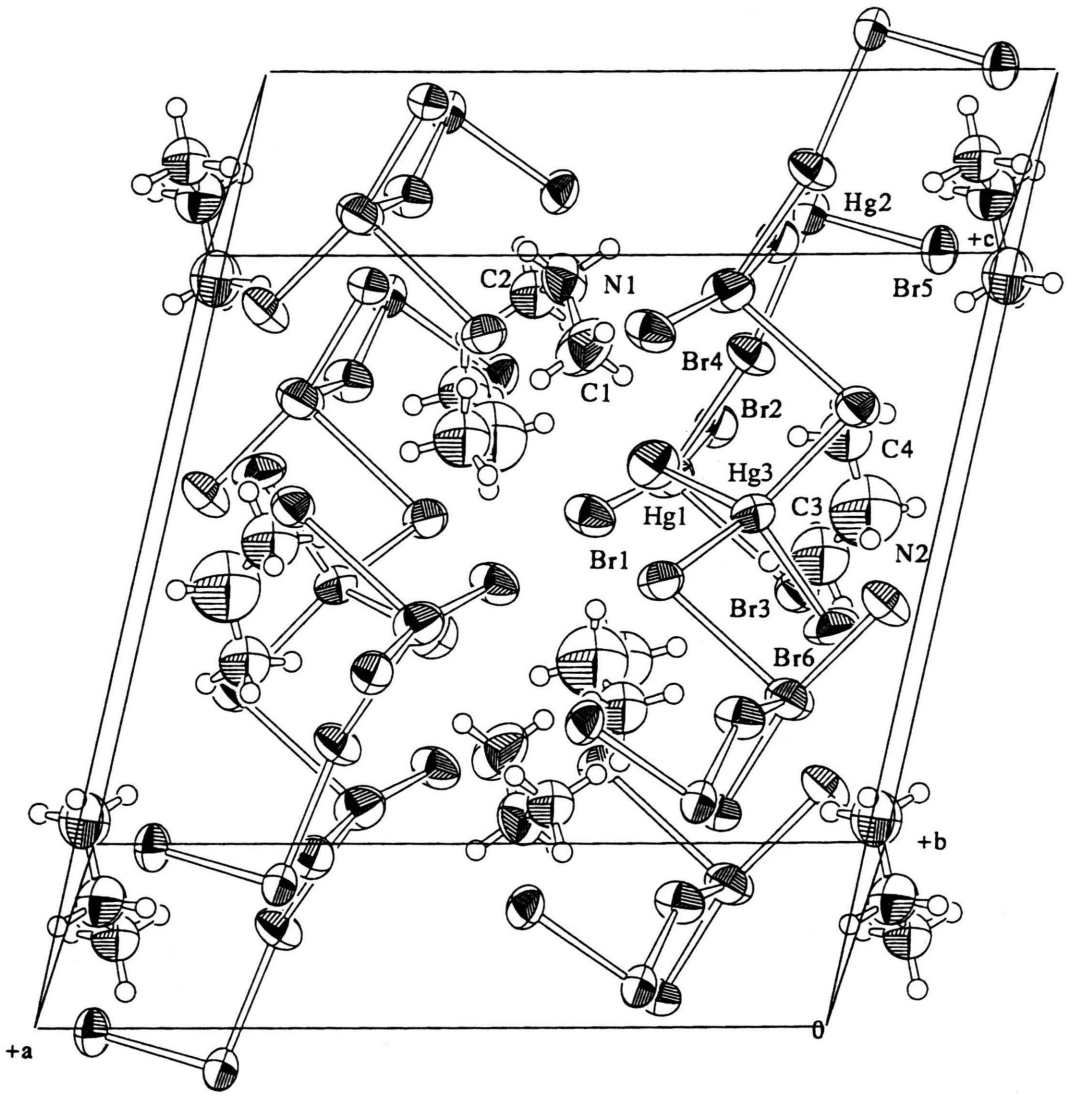

Fig. 9. The crystal structure of $(CH_3)_2NH_2HgBr_3$.

and 2.565 pm [10], and 101.75 and 87.05 MHz [11] for the terminal and the bridging Br atoms, respectively. These observations lead to a good correlation between the ^{81}Br NQR frequencies and the bond distances (and hence the coordination of Hg(II)) in a series of mercury halide complexes. A more elaborate investigation for such a correlation will be described elsewhere.

Phase Transitions and Structures of Phases I and III

The NQR spectrum of each phase at the phase transition temperature is shown in Fig. 11 as a stick diagram. In phase III, twelve resonance lines have been observed, which means that the number of nonequivalent Br atoms is doubled in phase III on the II-III phase transition. The change in the structure due to the transition seems to be slight, because the splitting pattern of the ^{81}Br NQR spectrum of phase II is almost identical to that of phase III. Thus, the basic structure of anion chains which consist of a $HgBr_2$ and two different $HgBr_4^{2-}$ anions may also be kept in the phase III. A possible idea to explain the ^{81}Br NQR spectrum of phase III (12 lines) is to assume that the 2-fold axis which exists

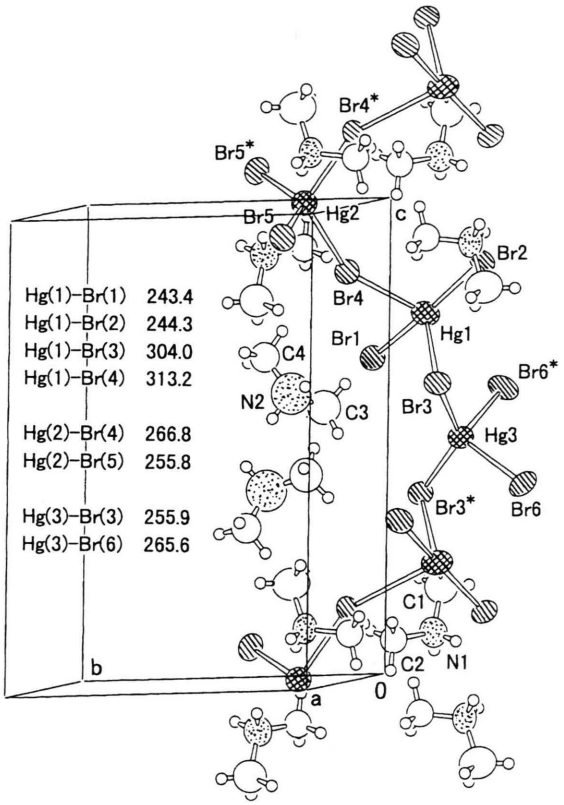

Fig. 10. The infinite chain of anions arranged almost in the c-direction. Hg2 and Hg3 are located on the two-fold axes. Br3 and Br3*, Br4 and Br4*, etc., are interconnected with the two-fold axes.

in phase II (6 lines) is lost to give a triclinic cell in phase III.

Contrary to the case of the III-II transition, the change in the ^{81}Br NQR spectrum due to the II-I transition is drastic (Fig. 11), suggesting that a considerable rearrangement of the Hg-Br bonds may occur at the transition. The nine ^{81}Br NQR lines in phase I are divided into two sets of the lower three and higher six lines which are largely different in frequency; the former and the latter sets may be assignable to bridging and terminal Br atoms, respectively. In connection with this observation it is worthwhile to examine the crystal structure of $(CH_3)_2NH_2HgCl_3$ ($P2_1/n$) [1]. This crystal contains a chain of anions consisting of three kinds of severely distorted $HgCl_4$ polyhedra which are interconnected with two long bridging and tow short terminal Hg-Cl bonds. There exist consequently six terminal and three bridging Cl atoms, which will just lead to an analogous chlorine NQR spectrum as the ^{81}Br NQR spectrum in phase I of $(CH_3)_2NH_2HgBr_3$, although the chlorine NQR spectrum is unfortunately unknown. Then, it seems very probable that phase I has the same structure as that of $(CH_3)_2NH_2HgCl_3$. One may notice that the chain of anions in phase I becomes similar to that in $(CH_3)_2NH_2HgCl_3$ by the elongation in the bridging Hg(3)-Br(3) and Hg(1)-Br(4) bonds and the shortening in the terminal Hg(2)-Br(5) and Hg(3)-Br(6) bonds. The supercooling of phase I, as well as the superheating of phase II can be attributed to the re-constructive nature of the transition accompanied by a considerable rearrangement of the Hg-Br bonds.

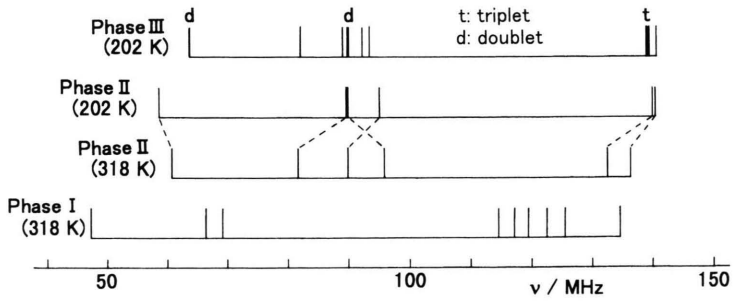

Fig. 11. The stick diagram of the ^{81}Br NQR spectrum for each phase of $(CH_3)_2NH_2HgBr_3$ at $T_{c2} = 202$ K and $T_{c1} = 318$ K, which is depicted with the frequency values obtained by inter- or extrapolating from the frequency *vs.* temperature curves.

[1] A. Ben Salah, J. W. Bats, H. Fuess, and A. Daoud, Inorg. Chim. Acta **63**, 169 (1982).
[2] I. Pabst, J. W. Bats, and H. Fuess, Acta Crystallogr. B **46**, 503 (1990).
[3] M. C. Burla, M. Camalli, G. Cascarano, C. Giacovazzo, G. Polidori, R. Spagna, and D. Viterbo, J. Appl. Crystallogr. **22**, 389 (1989).
[4] Molecular Structure Corporation. TEXAN. TEXRAY Structure Analysis Package. MSC, 3200 Research Forest Drive. The Woodslands. TX 77381, USA (1992).
[5] H. Terao, T. Okuda, A. Minami, T. Matsumoto, and Y. Takeda, Z. Naturforsch. **47a**, 99 (1992).
[6] H. Terao, T. Okuda, K. Koto, S. Dou, and Al. Weiss, Z. Naturforsch. **49a**, 202 (1994).
[7] H. Terao, T. Okuda, S. Uyama, H. Negita, S. Dou, H. Fuess, and Al. Weiss, Z. Naturforsch. **51a**, 1197 (1996).
[8] M. Körfer, H. Fuess, and J. W. Bats, Z. Anorg. Allg. Chem. **543**, 104 (1986).
[9] Terao *et al.*, unpublished results.
[10] M. Körfer, H. Fuess, J. W. Bats, and G. Klebe, Z. Anorg. Allg. Chem. **525**, 23 (1985).
[11] H. Terao and T. Okuda, Z. Naturforsch. **45a**, 343 (1990).